Dynamic estuarine Chlorophyll-a estimation-based time series harmonized Landsat- Sentinel images

Ha Thanh Tran[a]*, Hoa Thi Tran[b]*, Ngoc Minh Nguyen[c], Hai Minh Nguyen[a], Giang Truong Tran[b] and Phan Minh Thu[d]

[a] Department of Photogrammetry and Remote Sensing, Hanoi University of Mining and Geology, Dong Ngac, Hanoi, Vietnam
[b] Department of Geoinformatics, Hanoi University of Mining and Geology, Dong Ngac, Hanoi, Vietnam
[c] Vietnam National Space Centre, Vietnam Academy of Science and Technology, Hanoi, Vietnam
[d] Institute of Oceanography, Vietnam Academy of Science and Technology, Nha Trang 650000, Viet Nam

*Corresponding author. E-mail: tranthanhha@humg.edu.vn
ORCID: Ha Tran Thanh (0000-0003-2170-3007) ; Hoa Thi Tran (0000-0002-1742-0226) ; Ngoc Minh Nguyen. (0000-0001-5007-2641) ;Hai Minh Nguyen.(0009-0008-9794-4716) ;Giang Truong Tran; Phan Minh Thu (0000-0002-7394-0728)

ABSTRACT

This research develops a vigorous approach to estimate Chlorophyll-a (Chl-a) concentration in the dynamic, optically complex waters (or Case 2 water including coastal waters, estuaries and inland water bodies) of Ganh Rai Bay, Vietnam by leveraging time series harmonized Landsat and Sentinel-2 (TM-HLS) imagery. One of the fundamental challenges while conducting this method to compute Chl-a signal is noise caused by suspended sediments (TSS) and coloured dissolved organic matter (CDOM). Thus, the study utilizes spectral features (such as Blue/Green and Red/Green ratios) to correct TSS and CDOM interference, a critical step for Case 2 waters. Otherwise, by learning spectral correlation between different bands of the TM-HLS products and in-situ Chl-a lab-computed data, several log-transformed algorithms of selected bands were investigated to examine their efficiency in estimating Chl-a content. Results showed that the log-level regression model was the most effective which yielded a high coefficient of determination (R^2 = 0.888) and a minimal standard error (SE = 0.06). Furthermore, the spatial distribution analysis, utilizing the log-level model, revealed that the Chl-a concentration was highly variable in coastal area (13-15mg/m^3) due to river discharge and the semi-diurnal tidal regime, but

more stable offshore. The HLS data set is confirmed to be effective for continuous spatiotemporal water quality assessment.

Keywords: case 2 waters, chlorophyll-a, estuaries, TM-HLS, log-transformed algorithms, Vietnam.

HIGHLIGHTS

- Time series harmonized Landsat and Sentinel 2 (TM-HLS) data to achieve a much higher temporal resolution while maintain a consistent 30-meter spatial resolution for a long-term monitoring.
- Spectral correlation analysis between TM-HLS band reflectance and in-situ Chl-a lab computed content to nominate typical bands for further computation.
- Four log-transformed formulas of nominated bands were conducted to estimate Chl-a concentration.
- A validation between spectral estimated and in-situ computed was approached for indicating the most effective model which is the level-log regression.
- Series of maps were generated to examine spectral estimated Chl-a distribution over observation.

1. INTRODUCTION

Estuaries represent highly productive and ecologically significant transition zones between terrestrial and marine environments (Levin et al., 2001; Mateus et al., 2008). However, their critical function also renders them particularly susceptible to anthropogenic pressures, frequently leading to water quality degradation (Day Jr et al., 2012; Sato, 2010). Consequently, monitoring key biophysical indicators of water quality, such as chlorophyll-a (Chl-a) concentration, is paramount (Ferguson et al., 1996). Elevated Chl-a levels serve as a primary indicator of eutrophication and the potential formation of harmful algal blooms (HABs) (Cloern, 2019), which pose significant threats to estuarine health and ecosystem services (Peierls et al., 2003; Sin & Lee, 2020).

Practically, accurately and consistently measuring Chl-a in estuarine systems presents a persistent technical challenge (Maciel et al., 2023). One of major reasons is that estuaries are classified as optically complex "Case 2" waters, thus their inherent optical properties are not exclusively controlled by phytoplankton

(containing Chl-a but are also significantly influenced by other constituents) (Peierls et al., 2003). Additionally, these include high concentrations of suspended sediments, colored dissolved organic matter (CDOM), and, in shallow regions, bottom reflectance. As a result, this intricate mix of components makes it exceptionally difficult to isolate and accurately quantify the Chl-a spectral signature using satellite remote sensing (Le et al., 2013).

Otherwise, traditional *in-situ* sampling—collecting and laboratory-analyzing water samples—offers high accuracy but is inherently labor-intensive, expensive, and spatially and temporally constrained (Moses et al., 2009). This method cannot provide the continuous, synoptic coverage necessary to monitor the rapid, dynamic changes typical of estuarine environments (Chen et al., 2013).

While remote sensing provides a powerful alternative for broad spatial coverage, existing satellite missions have significant limitations (Le et al., 2013; Maciel et al., 2023; Yue et al., 2024):

- Firstly, constraints of temporal resolution: Free optical sensors like Landsat possess a long revisit period (16 days), which is often insufficient to capture the short-term, dynamic fluctuations in Chl-a driven by tidal cycles, episodic river discharge events, or fast-developing algal blooms.
- Secondly, limitations of spatial resolution: Conversely, some high-temporal resolution sensors may have a coarser spatial resolution (Moses et al., 2009), which fails to resolve the small-scale features and spatial heterogeneity characteristic of estuaries.

Therefore, the need for a high-frequency, high-resolution approach to consistently estimate Chl-a in dynamic, optically complex waters highlight a critical gap in current research. Several projects have worked on hamonized images (mixing different sensors at various spatial and temporal resolutions (Cao et al., 2022; Schaeffer et al., 2022). Cao et al. studied a robust solution lying in leveraging the complementary strengths of the Landsat and Sentinel-2 (S2) missions through spectral harmonization. By integrating data from both sensors into a unified, analysis-ready dataset (HLS), the limitations of individual missions can be effectively mitigated.

This harmonization approach provides two key benefits:

1. There is an enhancement of temporal frequency by combining the data streams drastically that increases the observational frequency to

approximately 2–3 days, enabling the effective capture of rapid, sub-weekly changes in Chl-a concentration.

2. Spatial resolution is consistent: The harmonized product maintains a reliable 30-meter spatial resolution, which is sufficient for resolving critical estuarine features.

Generally, the Chl-a concentration is derived from the water's spectral signature using log-transformed empirical equations applied to specific spectral band ratios. It is important to note, however, that the integration of Landsat 8/9 OLI and Sentinel-2 MSI data necessitates rigorous spectral harmonization. Hence, this is required to correct for subtle, yet significant, differences in the sensors' band configurations and spectral response functions (e.g., bandwidths and central wavelengths), ensuring a consistent and reliable long-term time series for continuous estuarine water quality assessment.

This research aims to establish and validate a robust methodology for continuous, high-spatiotemporal monitoring of Chl-a in complex estuarine environments using harmonized Landsat-Sentinel imagery. Specifically, the study seeks to answer the following questions:

1. To what extent can a spectrally time series harmonized Landsat and Sentinel-2 (TM- HLS) accurately and continuously estimate Chlorophyll-a concentrations in optically complex estuarine waters, and how does its performance compare to estimates derived from individual sensor data?
2. Which log-transformed spectral band ratio or empirically derived algorithm offers the most robust and spatially transferable estimation of Chl-a concentration across the diverse seasonal and physiochemical conditions within the study estuary?

Thus, by focusing on effectiveness of the TM – HLS, the research findings desire to establish and validate a robust methodology for the continuous, high-spatiotemporal monitoring Chl-a in particular and water quality assessment in general in complex estuarine environments.

2. MATERIALS AND METHODS

2.1 Study area

Ganh Rai Bay is a brackish water lagoon where several rivers such as Nga Bay River (Long Tau), Dong Tranh River, Thi Vai River and Dinh River flow into the basin from the north; to the east is Vung Tau peninsula with Nghinh Phong cape; to the

west is Can Thanh cape (Can Gio) with Dong Tranh cape, embracing the bay on three sides. Fig 1 below represents the study area.

Ganh Rai Bay is about 12km wide and about 21km long, corresponding to latitudes from 10º20'N to 10º30'N and longitudes from 106º50'E to 107º08'E. The tides in Ganh Rai Bay are irregular semi-diurnal, with water level fluctuations of about ±1.5m; the flow system depends on tides and wind regimes. In addition, the depth in the bay also changes in a complex way, significantly affecting the flow throughout the bay. Furthermore, due to its geographical location, Ganh Rai Bay is also of great significance in the waterway trade of goods in the Southeast region, especially Ho Chi Minh City. This is where many large rivers flow into the East Sea, so it is also a large fishing ground for aquatic products with many aquaculture farms such as shrimp, fish, clams, and oysters (Ba Ria - Vung Tau Department of Science and Technology, 2005).

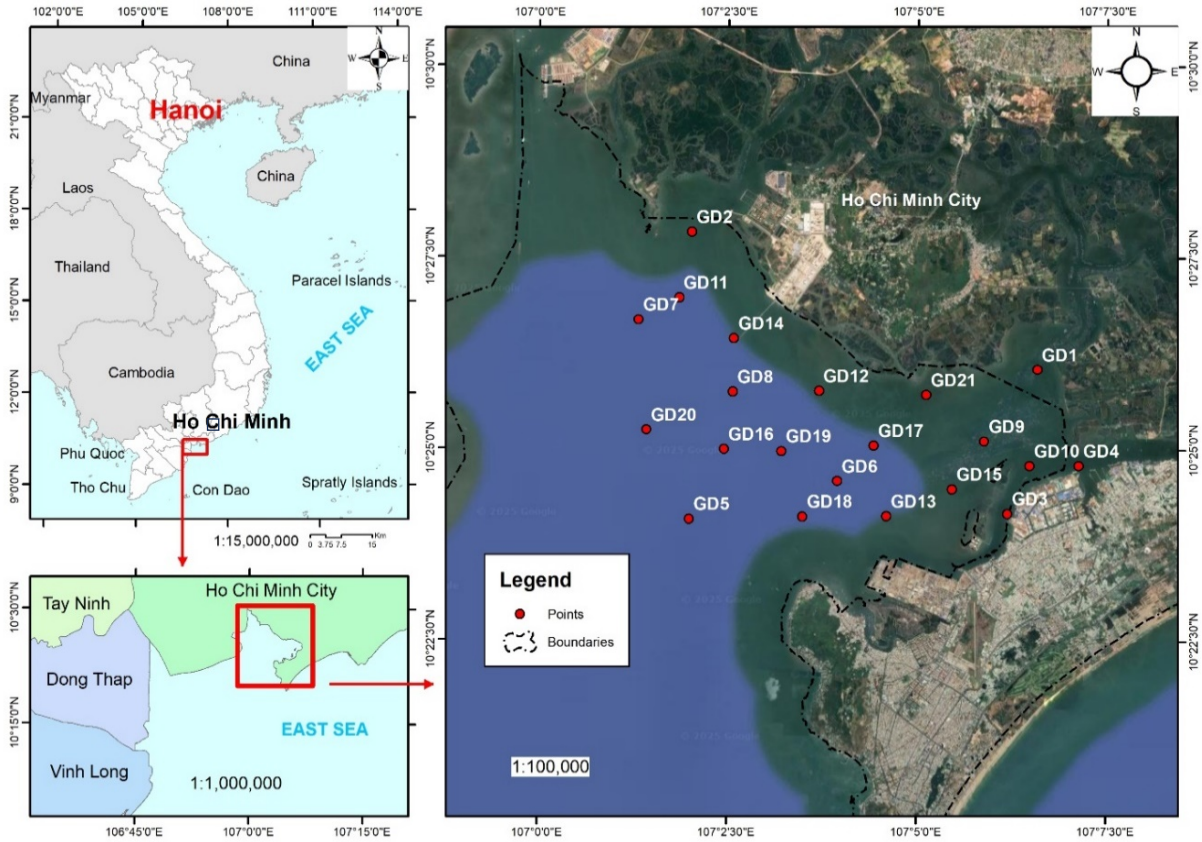

Fig 1.Study area, Ganh ai Bay

2.2. Data collection

The Landsat 8/9 and Sentinel-2 images which cover the study areas, are collected from USGS and ESA portals with cloud cover <30%, and specific bands that are available on Landsat 8/9 and Sentinel-2 images as Blue coastal (443nm), Blue

(490nm), Green (560nm), Red(665nm), NIR (865nm). The number of images is listed in table 1 below.

Although the amount of data collected is relatively large, however, due to the influence of meteorological conditions, the interruption of these individual data does not ensure continuous monitoring of water quality.

Table 1. Imagery dataset for the research

Types of image	Year	Number of scenes
Landsat 8/9	2020	12
(124053)	2021	10
	2022	19
	2023	14
	2024	19
Sentinel -2	2020	12
(T48PYS)	2021	11
	2022	11
	2023	9
	2024	12

As results, the harmonized images are used, the Harmonized Landsat and Sentinel-2 (HLS) project is a NASA initiative and collaboration with USGS to produce compatible surface reflectance (SR) data from a virtual constellation of satellite sensors, the Operational Land Imager (OLI) and Multi-Spectral Instrument (MSI) onboard the Landsat-8 and Sentinel-2 remote sensing satellites respectively. The combined measurement enables global land observation every 2-3 days at moderate (30 m) spatial resolution. The HLS project uses a set of algorithms to derive seamless products from OLI and MSI: atmospheric correction, cloud and cloud-shadow masking, spatial co-registration and common gridding, view angle normalization and spectral bandpass adjustment (Ju et al., 2025). The HLS data products can be regarded as the building blocks for a “data cube” so that a user may examine any pixel through time and treat the near-daily reflectance time series as though it came from a single sensor. These data are available through Earthdata Search as well as through NASA's Land Processes Distributed Active Archive Center (LP DAAC)

The in-situ data used in this study was collected through measurement stations in the area. The location of the stations is also shown in the Fig 1. The collected

data consists of 21 stations, of which 14 were used to build the model and 7 were used to test it.

2.3 Methods

In general, our methodology to assess Chl-a estimated model is divided into several steps.

Firstly, the TM-HLS dataset was collected from NASA LP DAAC via Google Earth Engine with Earth Engine Snippet *("NASA/HLS/HLSS30/v002").* In this study, the consistency between the reflectance values of Sentinel-2 and Landsat 8/9 images for each given spectral band was assessed by the mean absolute difference or MAD.

$$MAD = \frac{1}{n}\sum_{i=1}^{k} |R_{\lambda i}^{L} - R_{\lambda i}^{S}| \quad (1)$$

Where $R_{\lambda i}^{S}$ as Sentinel-2 reflectance value at location *i* in band *λ*

$R_{\lambda i}^{L}$ as Landsat 8/9 reflectance value at location *i* in band *λ*

n as the total number of survey points

After harmonization, spectral features were collected from R_{rs} to increase the sensitivity of the models to Chl-a changes, while minimizing the confounding effects of total suspended solids (TSS) and colored dissolved organic matter (CDOM), which are particularly dominant in estuarine waters such as Ganh Rai Bay. The feature collection followed established methods in bio-optical oceanography (Blondeau-Patissier et al., 2014; Gitelson, 1992; Hu et al., 2012), and included:

- *Reflectance values* of common bands (avaiable on Landsat 8/9 and Sentinel-2 images), including: Blue_coastal (443nm), Blue (490nm), Green (560nm), Red (665nm), NIR (865nm), which were used directly due to their relationship with phytoplankton absorption and backscatter properties.
- *Band ratios*: reduces illumination effects and emphasizes specific absorption properties. The ratio used is Blue /Green and Red /Green, which are the exact effective results in separating Chl-a from TSS in turbid water areas.

The approach is used to assess the independence of variables when estimating applied Pearson correlation (Deng et al., 2019), in which the correlation value *r* is divided into levels as shown in the following table 2.

Table 2: Correlation coefficient classification (Schober et al, 2018)

r	Interpretation
0.00 – 0.09	Negligible correlation
0.10 – 0.39	Weak correlation
0.40 – 0.69	Moderate correlation
0.70 – 0.89	Strong correlation
0.90 – 1.00	Very strong correlation

Next, in order to estimate Chl-a concentration, Logarithmic regression formulas were applied. The reason for this approach is that the relationship between Chl-a concentration and remote sensing reflectance is not linear (Menken et al., 2006), especially at high concentrations where the reflectance signal in the blue and green bands can become saturated. Thus, by taking the logarithm of the Chl-a concentration and the band ratio linearizes this relationship, making it possible to use a simple linear regression to derive the retrieval formula while effects of TSS and CDOM were corrected by using band ratio (Song et al., 2010).

In this study, four types of log transformation for multiple variables regression models are used to estimate Chl-a concentration from input data as reflectance, band ratios, such as:

$$\begin{aligned} &\text{Level-level regression: } y = b_0 + b_1x_1 + b_2x_2 + \ldots + b_kx_k \\ &\text{Log-level regression: } \ln y = b_0 + b_1x_1 + b_2x_2 + \ldots + b_kx_k \\ &\text{Level-log regression: } y = b_0 + b_1\ln x_1 + b_2\ln x_2 + \ldots + b_k\ln x_k \\ &\text{Log-log regression: } \ln y = b_0 + b_1\ln x_1 + b_2\ln x_2 + \ldots + b_k\ln x_k \end{aligned} \quad (2)$$

Finally, the most suitable model for the study area is selected based on determination coefficient value R^2, p-value, and to increase the reliability of the study, the standard error SE will also be considered. In which the determination coefficient value R^2 is divided into levels as shown in table 3 below.

Table 3: Determination coefficient classification (Moriasi et al., 2015)

R^2	Interpretation
≤ 0.5	Not Satisfactory
0.5 – 0.7	Satisfactory
0.7 – 0.8	Good
≥ 0.8	Very good

3 RESULTS

3.1 Consistency of data assessment

Before using the Sentinel-2 harmonized data to estimate Chl-a concentration to augment the Landsat data, there was an evaluation of the consistency of these

two types of images at the Blue, Green, Red, and NIR bands which were collected on the same day at the study area. The sampling location coincided with the survey location for in situ Chl-a concentration (see Fig. 1).

For the homogeneity assessment, Sentinel-2 and Landsat8/9 images were captured on the same day with cloud cover < 10%, ensuring that the sampling locations were not affected by clouds and cloud shadows. Among the data collected from 2020-2024, only the following dates met the requirements: January 17, 2021; April 7, 2021; June 21, 2022; February 11, 2024; March 22, 2024; November 17, 2024. To learn about correlation across respective bands of Landsat and Sentinel – 2 images, sample data were collected to examine. Graphs in Fig 2 illustrated the reflectance scatter plots of those spectral bands.

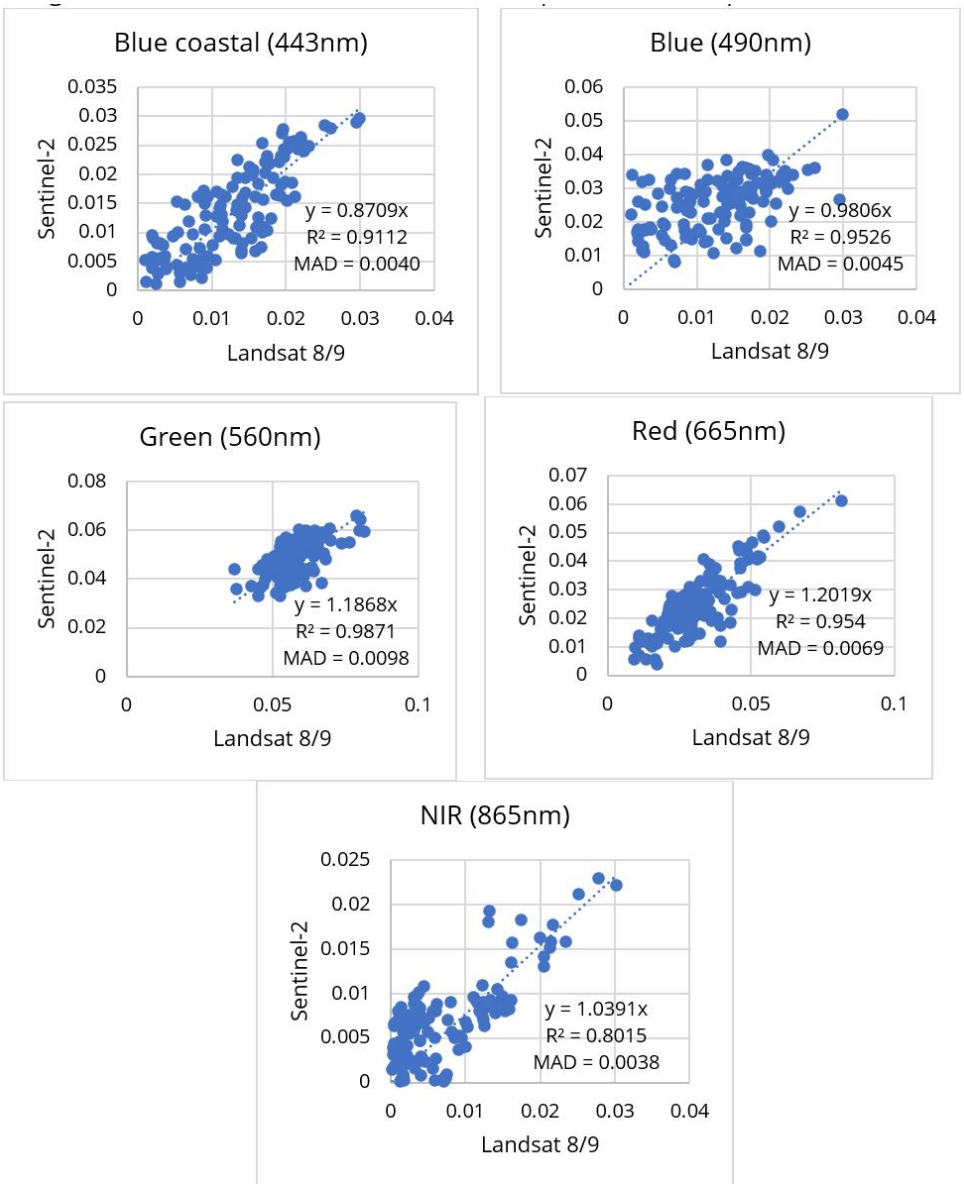

Fig 2: The reflectance scatter plots with Landsat 8/9 on the x- axis and Sentinel-2 on the y-axis, that show the consistency data in spectral bands as Blue coastal, Blue, Green, Red, NIR.

The correlation of reflectance values between the two types of data in the five bands is uneven, the highest R^2 coefficient is concentrated in the Green (0.9871), then Red (0.954), Blue (0.9526), Blue coastal (0.9112), and then the NIR channel (0.8015). However, if considering the consistency by MAD, this order is reversed, respectively NIR (0.0038), Blue coastal (0.0040), Blue (0.0045), Red (0.0069) and Green (0.0098). This is because the reflectance values at the NIR channel of the sampling points were much smaller than those of the other bands, especially the Green (see fig. 2). Most of the sampling points had reflectance values at the NIR band less than 0.01, while at the Green, these values were mostly bigger than 0.04. Therefore, it is understandable that the sensitivity to the amplitude of fluctuations is different and leads to the situation as mentioned above.

3.2 Estimation Chl-a concentration

To estimate Chl-a concentration in this study area, in situ data were collected at the time approximately closed to the acquisition of Sentinel-2 image T48PYS on 26/6/2022. Chl-a concentration was calculated using regression functions for four types of logarithmic transformations.

The correlation between in situ data (Chl-a) and the reflectance value of the image is shown in table 4. Although most of them are negative, when compared with the classification in table 4, most of the coefficients are strong, except the ratio Blue/Green is moderate. Thus, these variables can be used to estimate Chl-a concentration.

Table 4: Correlation coefficient between in situ data (Chl-a) and variables

	Blue coastal	*Blue*	*Green*	*Red*	*NIR*	*Red/Green*	*Blue/Green*	*Chl-a*
Blue coastal	1							
Blue	0.97	1						
Green	0.84	0.88	1					
Red	0.95	0.91	0.76	1				
NIR	0.89	0.87	0.61	0.96	1			
Red/Green	0.89	0.84	0.63	0.98	0.96	1		
Blue/Green	0.87	0.88	0.56	0.84	0.91	0.83	1	
Chl-a	-0.76	-0.76	-0.72	-0.79	-0.74	-0.76	-0.62	1

Each type of logarithmic transformation according to formula (2) above has the coefficients b_i determined for the input parameters which are reflectance values, spectral band ratio, spectral difference and then formula (2) will become:

Level-level regression model:

$$Chl-a = -72.956 * R_{rs}^{Bc} + 5827.38 * R_{rs}^{B} - 5971.95 * R_{rs}^{G} + 1760.36 * R_{rs}^{R} - 441.513 * R_{rs}^{N} - 373.823 * R_{rs}^{B/G} - 92.6523 * R_{rs}^{R/G} + 401.07$$

Log-level regression model:

$$Ln(Chl-a) = -2.9452 * R_{rs}^{Bc} + 325.813 * R_{rs}^{B} - 330.669 * R_{rs}^{G} + 90.8296 * R_{rs}^{R} - 25.1136 * R_{rs}^{N} - 20.9008 * R_{rs}^{B/G} - 4.6998 * R_{rs}^{R/G} + 24.0554$$

Level-log regression model:

$$Chl-a = 10.7612 * \ln\left(R_{rs}^{Bc}\right) + 6.4520 * \ln\left(R_{rs}^{B}\right) - 32.5949 * \ln\left(R_{rs}^{G}\right) + 9.7873 * \ln\left(R_{rs}^{R}\right) - 7.62859 * R_{rs}^{N} - 18.0678$$

Log-log regression model:

$$Ln(Chl-a) = 0.6321 * \ln\left(R_{rs}^{Bc}\right) + 0.2265 * \ln\left(R_{rs}^{B}\right) - 1.6569 * \ln\left(R_{rs}^{G}\right) + 0.5079 * \ln\left(R_{rs}^{R}\right) - 0.4215 * \ln\left(R_{rs}^{N}\right) + 0.9137$$

Then, the harmonized Landsat Sentinel (HLS) image was involved to estimate Chl-a with four logarithmic transformations, just like the individual Sentinel-2, and formula (2) will become:

Level-level regression model:

$$Chl-a = 296.2607 * R_{rs}^{Bc} - 2192.25 * R_{rs}^{B} + 969.5326 * R_{rs}^{G} - 870.416 * R_{rs}^{R} - 839.785 * R_{rs}^{N} + 84.8161 * R_{rs}^{B/G} + 71.2239 * R_{rs}^{R/G} - 32.3359$$

Log-level regression model:

$$Ln(Chl-a) = 16.6612 * R_{rs}^{Bc} - 131.132 * R_{rs}^{B} + 57.8338 * R_{rs}^{G} - 44.0288 * R_{rs}^{R} - 49.1933 * R_{rs}^{N} + 5.0416 * R_{rs}^{B/G} + 3.8336 * R_{rs}^{R/G} - 0.0549$$

Level-log regression model:

$$Chl-a = 15.1415 * \ln\left(R_{rs}^{Bc}\right) - 7.8266 * \ln\left(R_{rs}^{B}\right) - 4.8316 * \ln\left(R_{rs}^{R}\right) + 1.2231 * R_{rs}^{N} - 6.1564 * \ln\left(R_{rs}^{B/G}\right) + 32.6751$$

Log-log regression model:

$$Ln(Chl-a) = 0.891 * \ln\left(R_{rs}^{Bc}\right) - 0.3458 * \ln\left(R_{rs}^{B}\right) - 0.3151 * \ln\left(R_{rs}^{R}\right) + 0.0738 * \ln\left(R_{rs}^{N}\right) - 0.5153 * \ln\left(R_{rs}^{B/G}\right) + 3.9717$$

Where, R_{rs}^{Bc}, R_{rs}^{B}, R_{rs}^{G}, R_{rs}^{R}, R_{rs}^{N} are the reflectance of Blue coastal, Blue, Green, Red and NIR bands respectively

$R_{rs}^{B/G}$ is the ratio of reflectance of Blue band and Green band

$R_{rs}^{R/G}$ is the ratio of reflectance of Red band and Green band

Additionally, the selection of the most suitable model for each type of data (individual and harmonized) for each logarithm transformation model is evaluated based on three parameters: R^2, p-value, and SE. The results are shown in the following table 5.

Table 5: Comparing regression models with four logarithm transformation for Sentinel-2 original and harmonized

Model	*Individual Sentinel-2*			*HLS*		
	R^2	*p-value*	*SE*	*R^2*	*p-value*	*SE*
Level-level	0.86	0.028	1.06	0.87	0.023	1.02
Log-level	*0.88*	*0.021*	*0.06*	*0.88*	*0.020*	*0.06*
Level-log	0.77	0.114	1.38	0.86	0.027	1.05
Log-log	0.78	0.094	0.08	0.87	0.021	0.06

The R^2 values of the models were high and were in the range of good (0.7-0.8) and very good (>0.8), indicating high correlation with in situ data. However, for the two log-log and level-log models using the singular Sentinel-2 image, the p-values were higher than 0.05 (0.094 and 0.114, respectively), which means that these two models were worthless. In the other models, the p-values were all significant, but when considering the standard error SE, only the log-level model had the smallest SE value, which means that this model best represented the overall Chl-a concentration.

Furthermore, the log-level model used to estimate Chl-a content, was verified by 7 sampling points; and the RMSE value was used to evaluate the accuracy of the model. The RMSE for the singular and harmonized Landsat Sentinel-2 images are 2.32 and 2.73, respectively. The results illustrated in Fig 3 show that: although the log-level model of both cases is good with a similarity of R^2, p-value, SE values, but when calculating, the Chl-a value of the harmonized image is higher (about 5%) than the individual image. The reason is explained that the harmonized image has been recalculated with the spectral value approaching the spectral reflectance value of the Landsat 8/9 image.

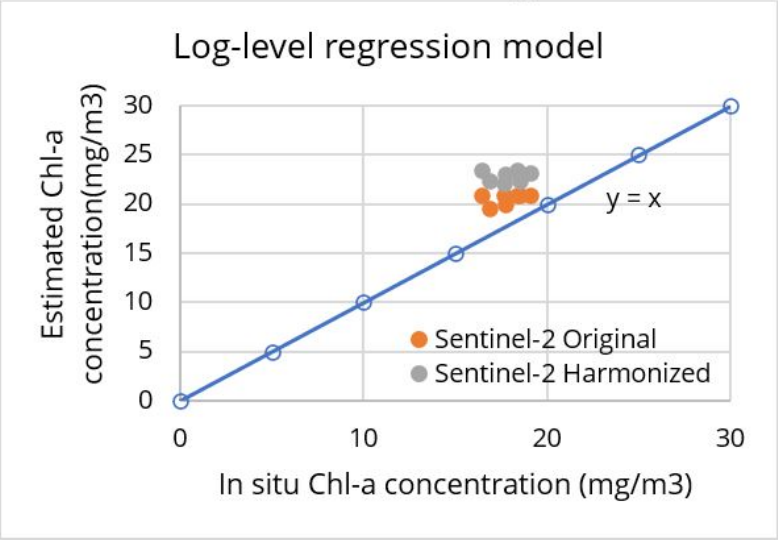

Fig 3: Comparison of the estimated values from Sentinel-2 (original and harmonized or HLS and in situ Chl-a concentration

3.3 Spatial-temporal distribution in Chl-a concentration

Remote sensing reflectance (R_{rs}) products derived from satellite imagery provide indirect proxies for chlorophyll-a (Chl-a) concentration, but their accuracy is highly dependent on the optical complexity of the study area. In estuarine and coastal waters such as Ganh Rai Bay (Ho Chi Minh City), high levels of total suspended solids (TSS), colored dissolved organic matter (CDOM), and nutrient influxes from riverine discharge led to the case-II water conditions, where conventional global ocean-color algorithms tend to underperform (Morel & Prieur, 1977; Sathyendranath, 2000). Therefore, regional calibration is essential to adapt bio-optical models to the specific environmental and optical properties of the study site.

The spatial distribution of Chl-a content in Ganh Rai Bay area in dry seasons and rainy seasons is shown in Fig 4 below. In particular, the Chl-a content between the two seasons is most clearly shown in coastal areas (lime to yellow), the fluctuation here is up to 10mg/m^3, when in the dry season the value fluctuates between 13-15mg/m^3 and in the rainy season it is between 23-25mg/m^3. The area, where is far from the coast has a fairly stable Chl-a content and fluctuates between 19-22mg/m^3, the main reason is that this area has a fairly large depth of about 7-8m and a relatively flat bottom terrain.

In the east of the area, where the Cha Va River flows from the North, the presence of aquaculture cages near the estuary near the bay is clearly visible. This area has Chl-a content ranging from 17-19mg/m^3 and is quite stable in both the rainy and dry seasons.

The study area is affected by the semi-diurnal tide regime with sea level fluctuations of about ± 1.5m, in addition, the acquisition time of the Sentinel-2 and Landsat8/9 satellites is around 10am, which is the time when there is a change in water level. All these factors affect the fluctuation of Chl-a concentration. For example, on January 27, 2024, February 26, 2024, and April 11, 2024, at 10am., the tide level was 0.8m, 1.31m, and 2.02m, respectively (https://thuydacvietnam.org.vn/thuy-trieu/); the Chl-a concentration at the observation location on January 27, 2024, and February 26, 2024 was in the range of 14.3 - 15.3 mg/m3, and on April 11, 2024, it was 17.3 mg/m3. The water level changed the turbidity in the coastal area, leading to a change in the Chl-a concentration.

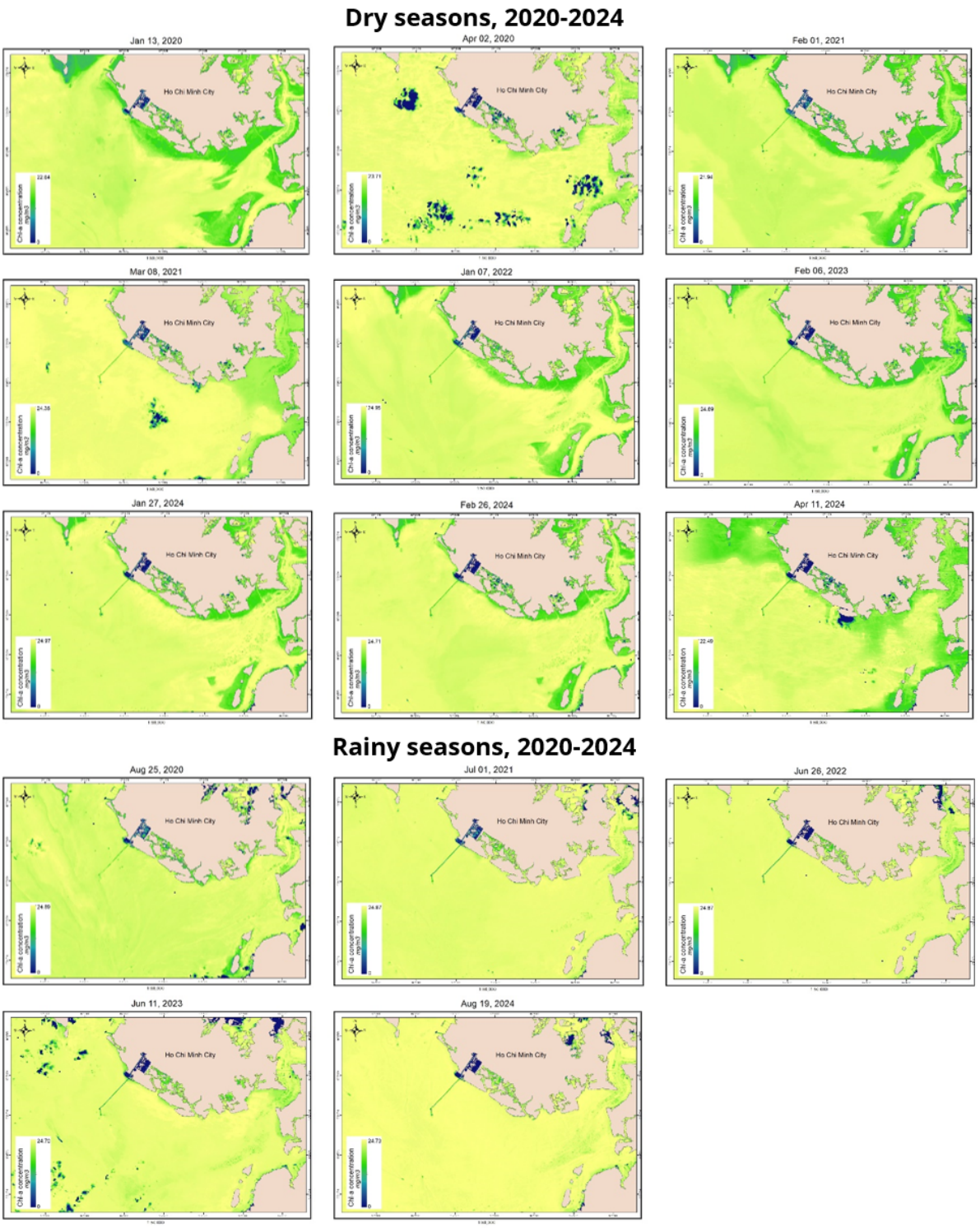

Fig 4: The spatial distribution of Chl-a concentration in Ganh Rai Bay in the dry seasons (above) and the rainy seasons (below)

4 DISCUSSIONS & CONCLUSIONS

Based on Chl-a data from field measurements and R_{rs} obtained on individual Sentinel-2, Harmonized Landsat - Sentinel-2, the study built a local model (log- log

algorithm) to monitor Chl-a concentration in Ganh Rai Bay. Chl-a concentration was estimated according to the log-level logarithm transformation model with R^2 = 0.88 and the RMSE for the both images are 2.32 and 2.73, respectively. Thus, the study specifically demonstrated that the spectrally time series harmonized Landsat Sentinel 2 data significantly enhances the accuracy and continuity of Chl-a concentration estimates in optically complex estuarine waters compared to estimates derived from individual Sentinel 2 alone. The research method in this paper has the potential to be used for water quality monitoring in some such coastal areas.

The spatial distribution of Chl-a in Ganh Rai Bay was duly affected by the discharge from Cha Va and Dinh rivers and tended to decrease from shore to offshore. Chl-a concentrations tended to be stable between the two seasons of the year while the differences mainly came from the shore area, which is strongly influenced by human activities and the semi-diurnal tidal regime in the area. The HLS data can be potentially used to assess the spatio-temporal distribution of Chl-a concentrations.

Furthermore, the investigation identified that a log-transformed spectral band ratio involving the red and near-infrared bands offered the most robust and spatially transferable empirical algorithm for Chl-a estimation. This specific algorithm maintained high predictive power across the diverse seasonal and physiochemical conditions encountered within the study estuary. These findings affirm the utility of sensor harmonization for long-term water quality assessment, providing resource managers with a reliable, high-frequency tool essential for tracking ecological shifts and mitigating the impacts of eutrophication in dynamic coastal systems. Additionally, the harmonized data offers advantages from enabling consistent multi-sensor time series analysis; minimizing TSS and CDOM noise through band ratios and indexes; and providing a diverse feature set for machine learning models (e.g., Ridge Regression, or Random Forests) to select the most appropriate predictors. Although there are limitations, such as the possibility of multicollinearity, especially in band ratios, and leading to the reduced performance of classical OC algorithms in estuarine waters, these limitations are addressed through the application of Ridge Regression or Random Forests in the next study.

ACKNOWLEDGEMENTS

We acknowledge the research project B2025 MDA05 for dataset and methodology development.

AUTHOR CONTRIBUTIONS

Conceptualization: Ha Tran Thanh, Hoa Thi Tran

Methodology: Hoa Thi Tran, Ha Tran Thanh, Phan Minh Thu

Data processing and analysis: Hai Minh Nguyen, Giang Truong Tran, Ngoc Minh Nguyen

Writing – drafting, reviewing, editing: Hoa Thi Tran, Ha Tran Thanh

Supervision: Ha Tran Thanh, Phan Minh Thu

REFERENCES

Blondeau-Patissier, D., Gower, J. F., Dekker, A. G., Phinn, S. R., & Brando, V. E. (2014). A review of ocean color remote sensing methods and statistical techniques for the detection, mapping and analysis of phytoplankton blooms in coastal and open oceans. *Progress in oceanography*, *123*, 123-144.

Cao, Z., Ma, R., Liu, M., Duan, H., Xiao, Q., Xue, K., & Shen, M. (2022). Harmonized chlorophyll-a retrievals in inland lakes from Landsat-8/9 and Sentinel 2A/B virtual constellation through machine learning. *IEEE Transactions on Geoscience and Remote Sensing*, *60*, 1-16.

Chen, J., Zhang, M., Cui, T., & Wen, Z. (2013). A review of some important technical problems in respect of satellite remote sensing of chlorophyll-a concentration in coastal waters. *IEEE Journal of Selected Topics in Applied Earth Observations and Remote Sensing*, *6*(5), 2275-2289.

Cloern, J. E. (2019). Patterns, pace, and processes of water-quality variability in a long-studied estuary. *Limnology and Oceanography*, *64*(S1), S192-S208.

Day Jr, J. W., Yáñez-Arancibia, A., Kemp, W. M., & Crump, B. C. (2012). Introduction to estuarine ecology. *Estuarine ecology*, 1-18.

Deng, J., Chen, F., Hu, W., Lu, X., Xu, B., & Hamilton, D. P. (2019). Variations in the distribution of Chl-a and simulation using a multiple regression model. *International Journal of Environmental Research and Public Health*, *16*(22), 4553.

Ferguson, C. M., Coote, B. G., Ashbolt, N. J., & Stevenson, I. M. (1996). Relationships between indicators, pathogens and water quality in an estuarine system. *Water Research*, *30*(9), 2045-2054.

Gitelson, A. (1992). The peak near 700 nm on radiance spectra of algae and water: relationships of its magnitude and position with chlorophyll concentration. *International journal of remote sensing*, *13*(17), 3367-3373.

Hu, C., Lee, Z., & Franz, B. (2012). Chlorophyll aalgorithms for oligotrophic oceans: A novel approach based on three-band reflectance difference. *Journal of Geophysical Research: Oceans*, *117*(C1).

Ju, J., Zhou, Q., Freitag, B., Roy, D. P., Zhang, H. K., Sridhar, M., Mandel, J., Arab, S., Schmidt, G., & Crawford, C. J. (2025). The Harmonized Landsat and Sentinel-2 version 2.0 surface reflectance dataset. *Remote sensing of Environment*, *324*, 114723.

Le, C., Hu, C., English, D., Cannizzaro, J., & Kovach, C. (2013). Climate-driven chlorophyll-a changes in a turbid estuary: Observations from satellites and implications for management. *Remote sensing of Environment*, *130*, 11-24.

Levin, L. A., Boesch, D. F., Covich, A., Dahm, C., Erséus, C., Ewel, K. C., Kneib, R. T., Moldenke, A., Palmer, M. A., & Snelgrove, P. (2001). The function of marine critical transition zones and the importance of sediment biodiversity. *Ecosystems*, *4*(5), 430-451.

Maciel, F. P., Haakonsson, S., Ponce de León, L., Bonilla, S., & Pedocchi, F. (2023). Challenges for chlorophyll-a remote sensing in a highly variable turbidity estuary, an implementation with sentinel-2. *Geocarto International*, *38*(1), 2160017.

Mateus, M., Mateus, S., & Baretta, J. (2008). Basic concepts of estuarine ecology. *Perspect. Integr. Coast. Zone Manag. South Am*, *10*(2.1), 4497.0562.

Menken, K. D., Brezonik, P. L., & Bauer, M. E. (2006). Influence of chlorophyll and colored dissolved organic matter (CDOM) on lake reflectance spectra: Implications for measuring lake properties by remote sensing. *Lake and Reservoir Management*, *22*(3), 179-190.

Morel, A., & Prieur, L. (1977). Analysis of variations in ocean color 1. *Limnology and Oceanography*, *22*(4), 709-722.

Moriasi, D. N., Gitau, M. W., Pai, N., & Daggupati, P. (2015). Hydrologic and water quality models: Performance measures and evaluation criteria. *Transactions of the ASABE*, *58*(6), 1763-1785.

Moses, W. J., Gitelson, A. A., Berdnikov, S., & Povazhnyy, V. (2009). Estimation of chlorophyll-a concentration in case II waters using MODIS and MERISdata—successes and challenges. *Environmental research letters*, *4*(4), 045005.

Peierls, B. L., Christian, R. R., & Paerl, H. W. (2003). Water quality and phytoplankton as indicators of hurricane impacts on a large estuarine ecosystem. *Estuaries*, *26*(5), 1329-1343.

Sathyendranath, S. (2000). Remote sensing of ocean colour in coastal, and other optically-complex, waters.

Sato, M. (2010). Anthropogenic decline of the peculiar fauna of estuarine mudflats in Japan. *Plankton and Benthos Research*, *5*(Supplement), 202-213.

Schaeffer, B., Salls, W., Coffer, M., Lebreton, C., Werther, M., Stelzer, K., Urquhart, E., & Gurlin, D. (2022). Merging of the Case 2 Regional Coast Colour and Maximum-Peak Height chlorophyll-a algorithms: validation and demonstration of satellite-derived retrievals across US lakes. *Environmental Monitoring and Assessment*, *194*(3), 179.

Sin, Y., & Lee, H. (2020). Changes in hydrology, water quality, and algal blooms in a freshwater system impounded with engineered structures in a temperate monsoon river estuary. *Journal of Hydrology: Regional Studies*, *32*, 100744.

Song, K., Liu, D., Li, L., Wang, Z., Wang, Y., & Jiang, G. (2010). Spectral absorption properties of colored dissolved organic matter (CDOM) and total suspended matter (TSM) of inland waters. Atmospheric and Environmental Remote Sensing Data Processing and Utilization VI: Readiness for GEOSS IV,

Yue, L., Zhang, L., Peng, R., Zeng, C., Duan, H., & Shen, H. (2024). Understanding the potential, uncertainties, and limitations of spatiotemporal fusion for monitoring chlorophyll a concentration in inland Eutrophic Lakes. *Journal of Remote Sensing*, *4*, 0209.

Ba Ria - Vung Tau Department of Science and Technology (2005), Report of project "Research on the design of the environmental monitoring network in Ba Ria- Vung Tau Province and the development of support tool on the digital map".

https://thuydacvietnam.org.vn/thuy-trieu/

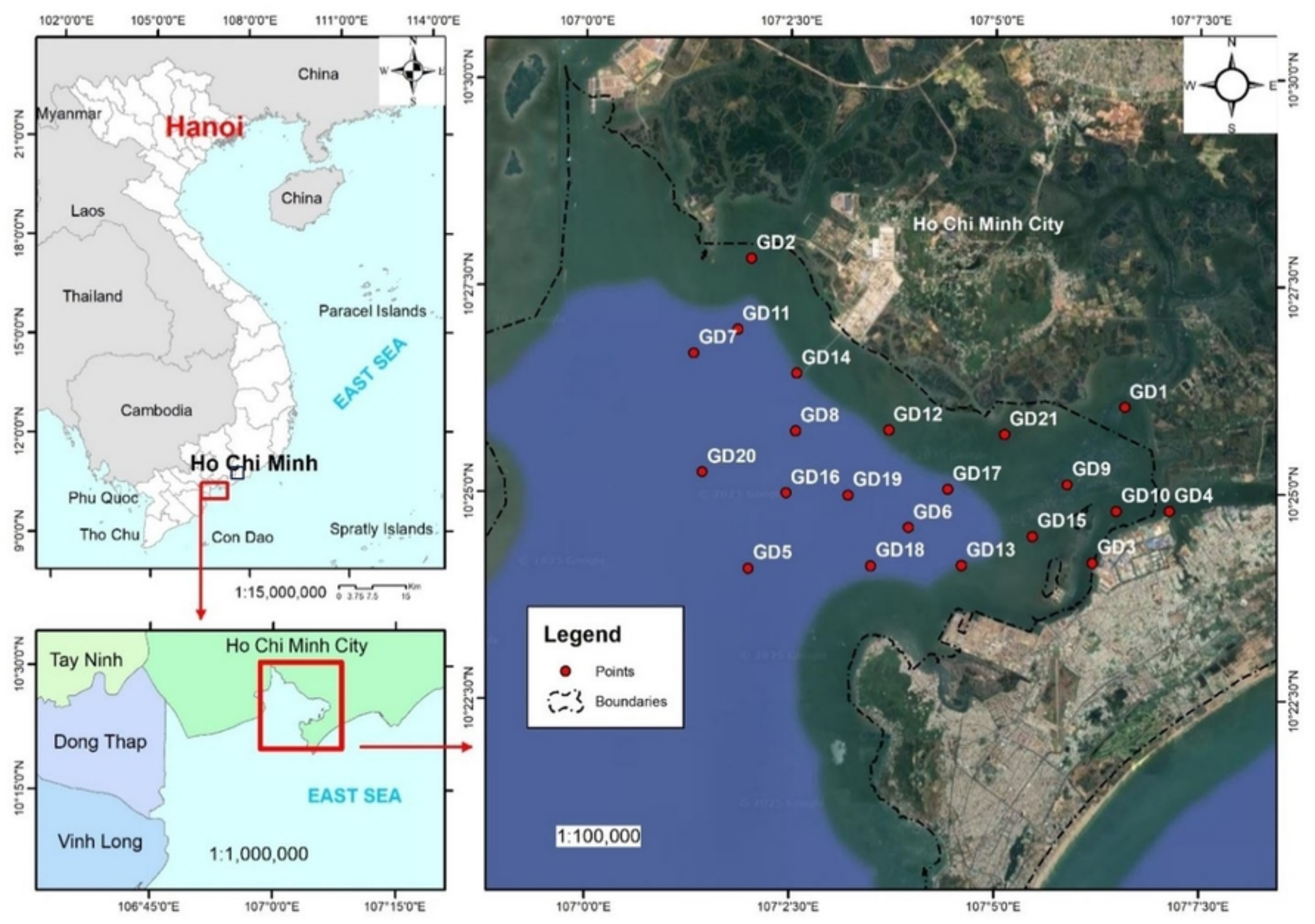
China
Myanmar
Hanoi
China
Laos
Thailand
Paracel Islands
EAST SEA
Cambodia
Ho Chi Minh
Phu Quoc
Tho Chu
Con Dao
Spratly Islands
1:15,000,000
Tay Ninh
Ho Chi Minh City
Dong Thap
EAST SEA
Vinh Long
1:1,000,000
Ho Chi Minh City
GD2
GD11
GD7
GD14
GD1
GD8
GD12
GD21
GD20
GD16
GD19
GD17
GD9
GD10
GD4
GD6
GD15
GD5
GD18
GD13
GD3
Legend
Points
Boundaries
1:100,000

Fig 1

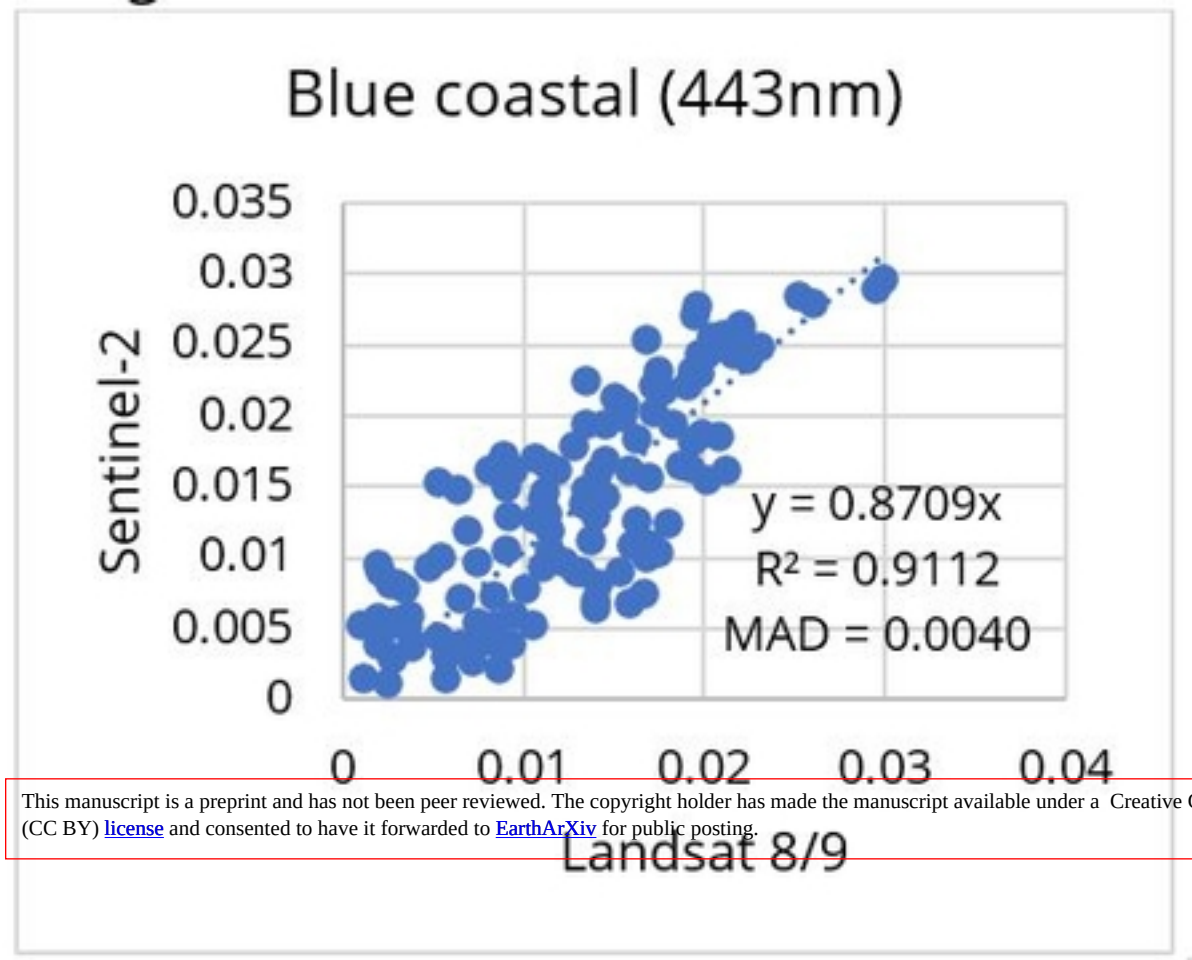

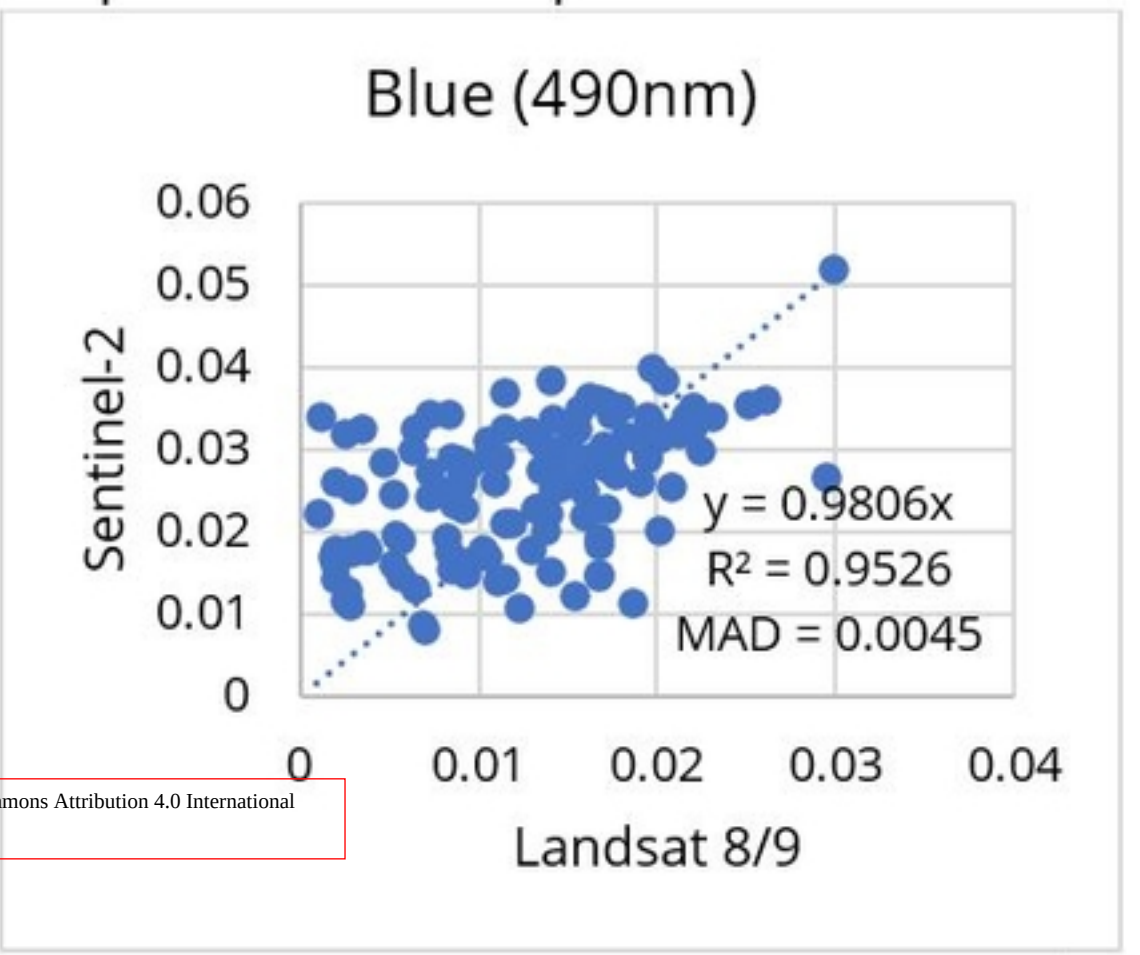

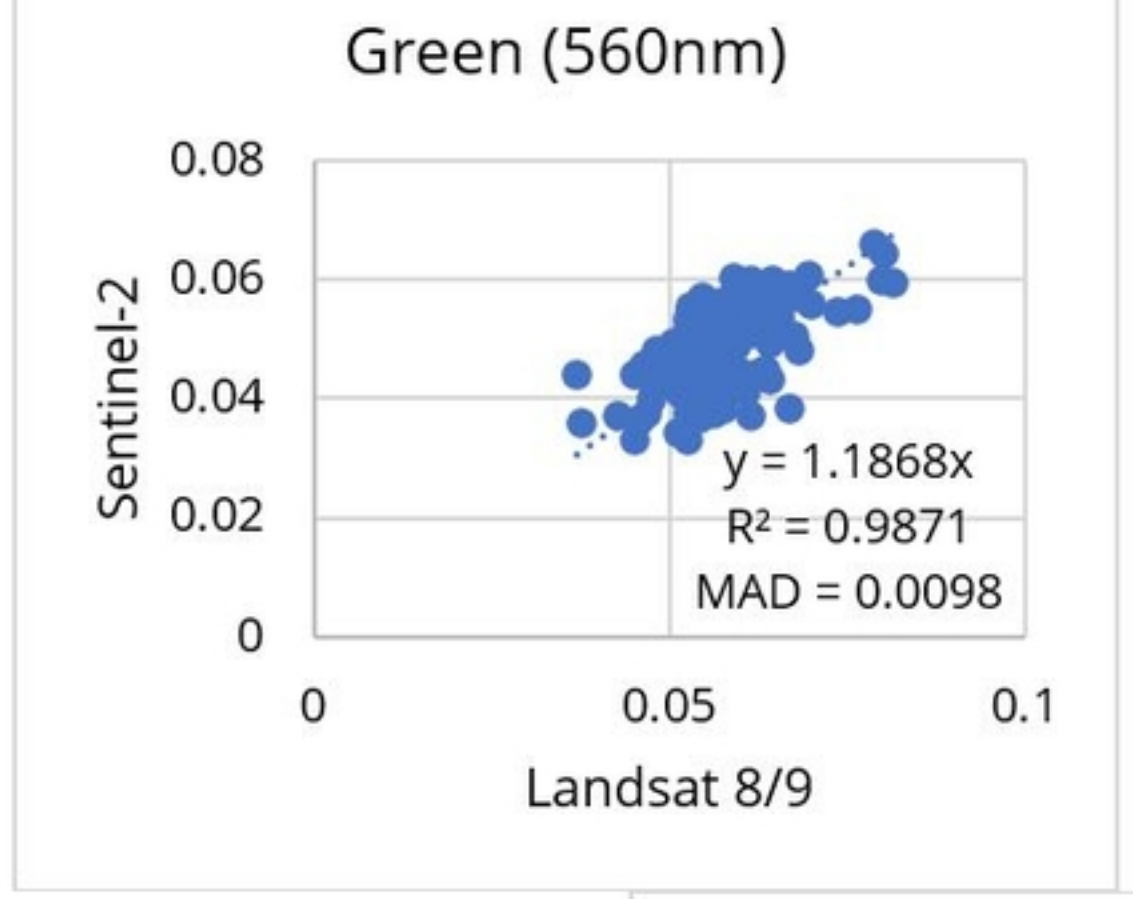

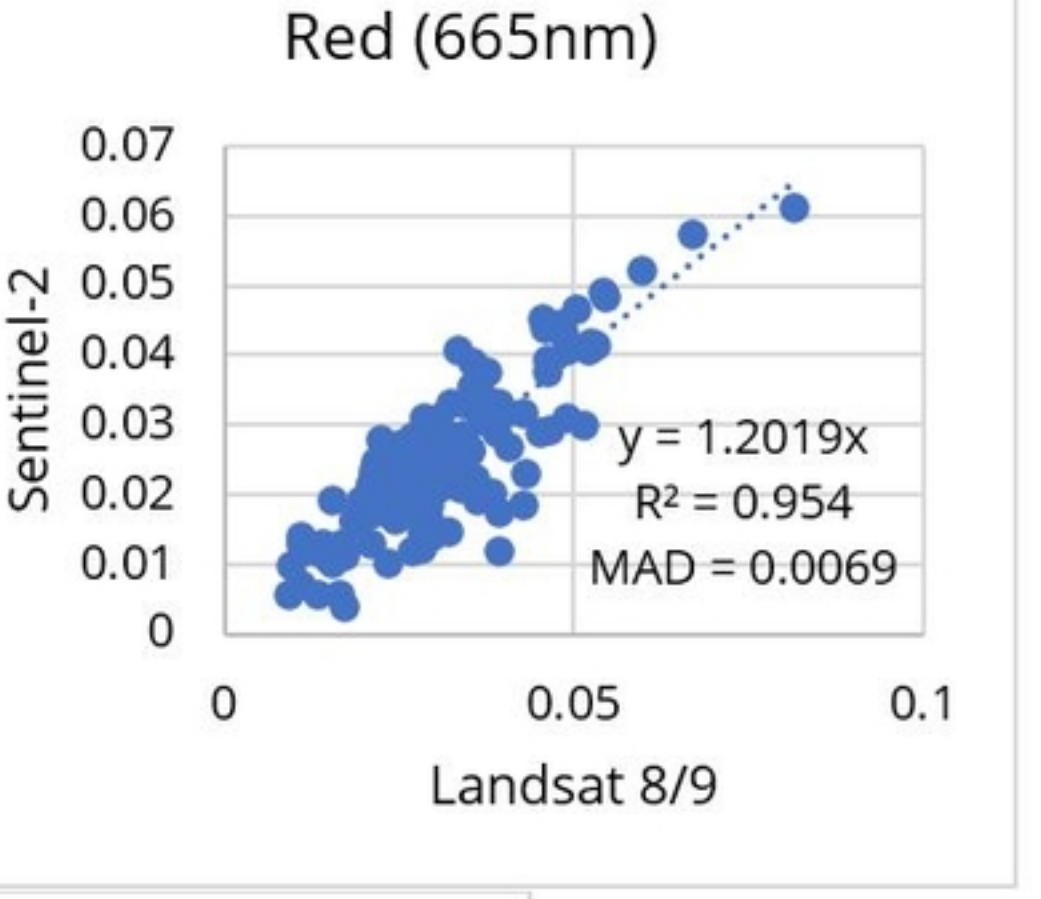

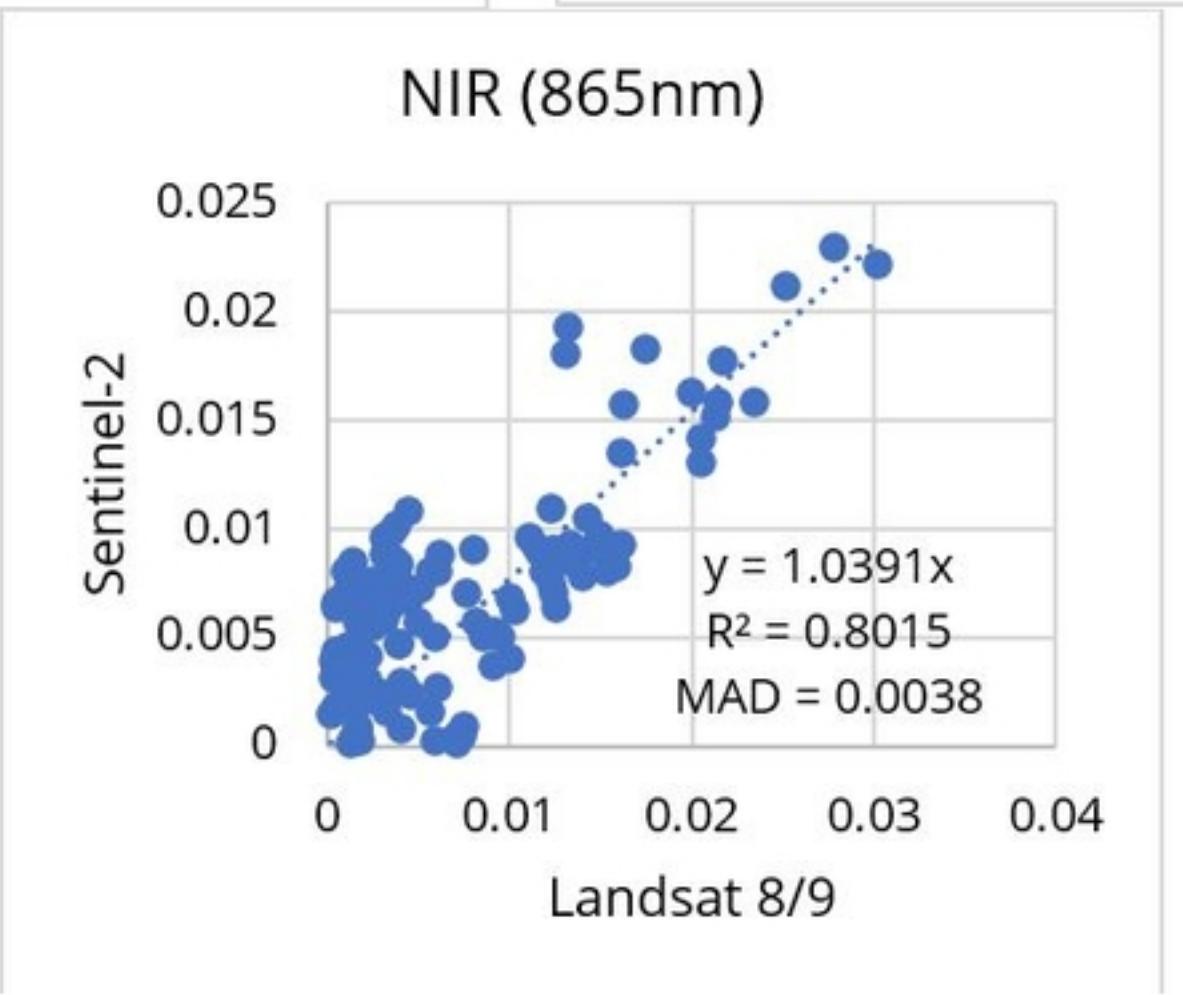

Fig 2

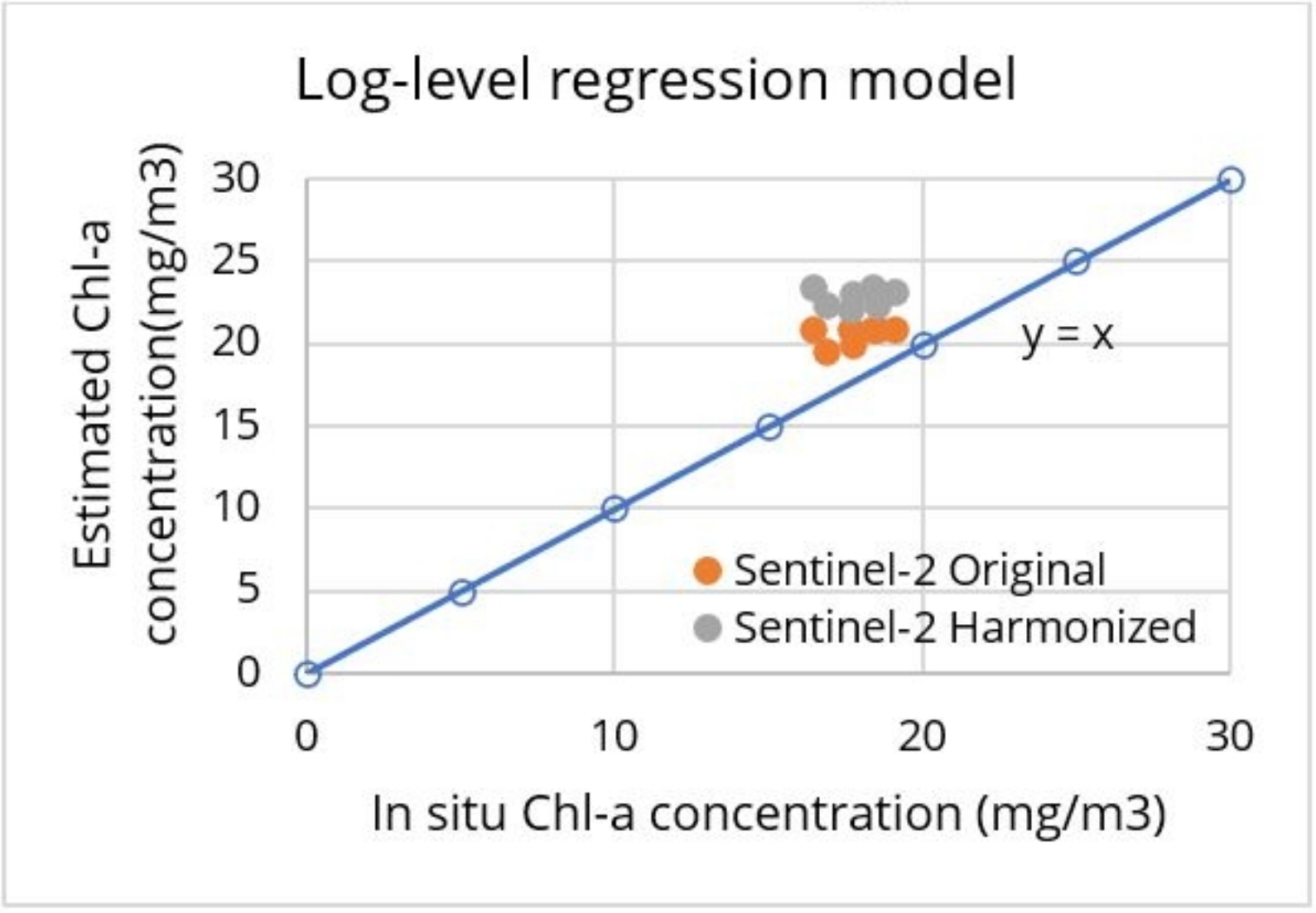
Log-level regression model
Estimated Chl-a concentration(mg/m3)
30
25
20
15
10
5
0
0
10
20
30
In situ Chl-a concentration (mg/m3)
y = x
Sentinel-2 Original
Sentinel-2 Harmonized

Fig 3

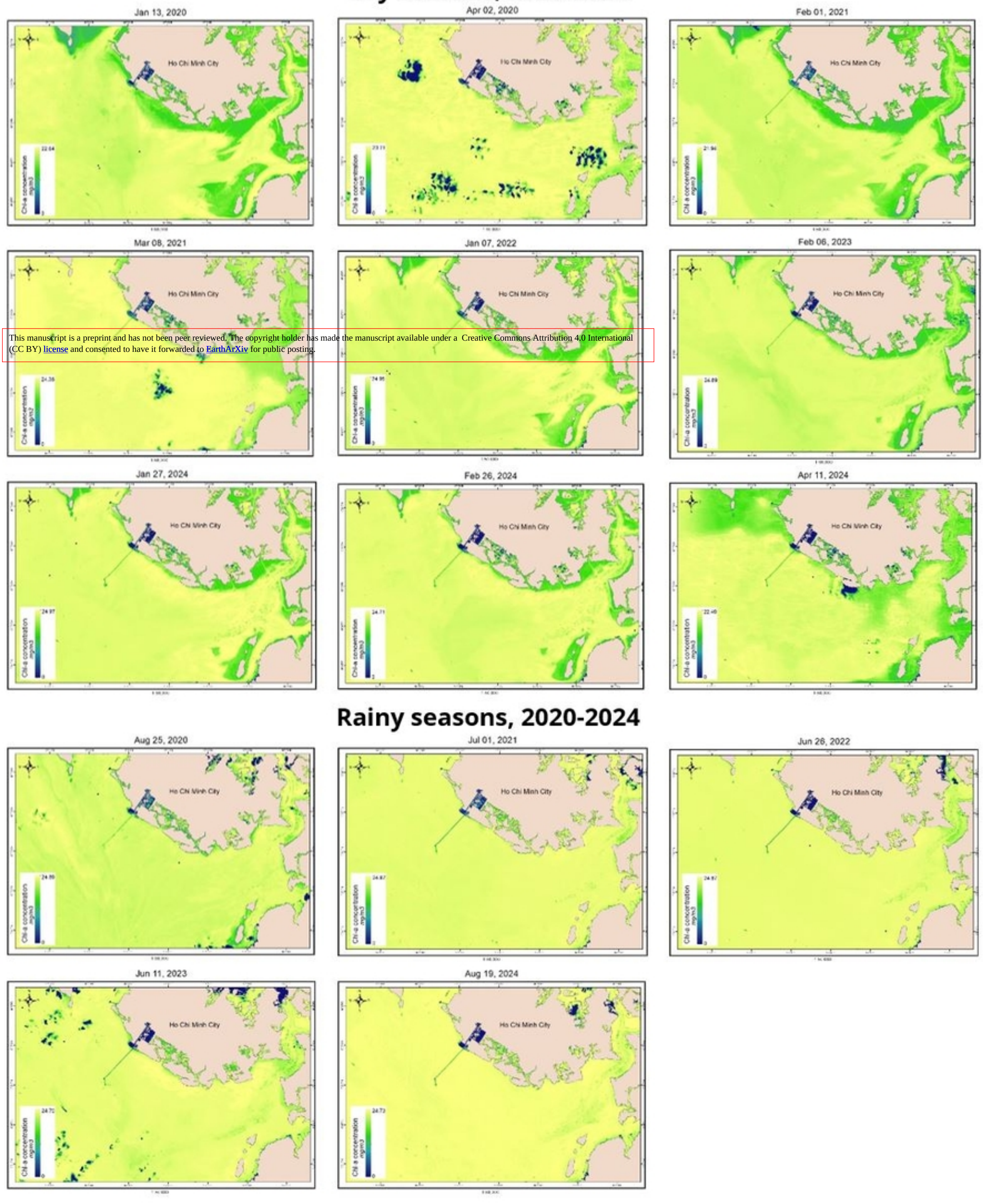

Fig 4